A generalized coherence framework for detecting and characterizing nonlinear interactions in the nervous system

Yang, Yuan; Solis Escalante, Teodoro; van der Helm, Frans; Schouten, Alfred

Important note
To cite this publication, please use the final published version (if applicable).
Please check the document version above.

A Generalized Coherence Framework for Detecting and Characterizing Nonlinear Interactions in the Nervous System

Yuan Yang[*], Teodoro Solis-Escalante, *Member, IEEE*, Frans C.T. van der Helm, and Alfred C. Schouten

Abstract — Objective: **This paper introduces a generalized coherence framework for detecting and characterizing nonlinear interactions in the nervous system, namely *cross-spectral coherence* (CSC). CSC can detect different types of nonlinear interactions including harmonic and intermodulation coupling as present in static nonlinearities and also subharmonic coupling, which only occurs with dynamic nonlinearities.** *Methods:* **We verified the performance of CSC in model simulations with both static and dynamic nonlinear systems. We applied CSC to investigate nonlinear stimulus-response interactions in the human proprioceptive system. A periodic movement perturbation was imposed to the wrist when the subjects performed an isotonic wrist flexion. CSC analysis was performed between the perturbation and brain responses (EEG).** *Results:* **Both the simulation and the application demonstrated that CSC successfully detected different types of nonlinear interactions. High-order nonlinearities were revealed in the proprioceptive system, shown in harmonic and intermodulation coupling between the perturbation and EEG for all subjects. Subharmonic coupling was found in some subjects but not all.** *Conclusion:* **This work provides a general tool to detect and characterize nonlinear nature and dynamics of the nervous system. The application of CSC on the experimental dataset indicates a complex nonlinear dynamics in the proprioceptive system.** *Significance:* **This novel framework 1) unveils the nonlinear neural dynamics in a more complete way than the existing coherence measures, and 2) is more suitable for estimating the input-output relation regarding both phase and amplitude compared to phase synchrony measures (which only consider phase coupling). Subharmonic coupling is reported in human proprioceptive system for the first time.**

Index Terms— **Coherence, cross-frequency coupling, EEG, human proprioceptive system, nonlinear dynamics.**

I. INTRODUCTION

Nervous systems are highly nonlinear [1-3]. They can present different forms of nonlinear interaction between an input (stimulus) and the corresponding output (neural response), such as harmonic, subharmonic and/or intermodulation coupling. Assessing the nonlinear interaction between stimulus and neural response is essential for a better understanding of the nervous system and could be useful for clinically related purposes, such as investigating motor disorders [4], migraine [5] and epilepsy [6].

Steady-state sensory stimulations, such as visual flicker and tactile vibration, typically evoke brain responses in harmonics [7, 8], i.e. integer multiples of a stimulus frequency (e.g. $3f_1$), and intermodulation frequencies [9, 10], i.e. integer combinations of the stimulus frequencies (e.g. $3f_2 - 2f_1$). A simple static nonlinear system, such as the power function, can generate these two types of nonlinear coupling. Subharmonic coupling, where the output frequency is a fraction of an input frequency, e.g. $f_1/2$, has been reported in a few studies mainly for visual systems (e.g. [7]). Recently, Langdon and colleagues found subharmonic coupling between tactile vibration and brain responses (electroencephalogram, EEG) [11]. Subharmonic coupling represents a more complex type of nonlinearity than harmonic and intermodulation coupling [12], and it is known to be associated with intrinsic nonlinear dynamics in the human brain [3, 11].

The interactions between sensory stimuli and brain responses can be studied by various approaches in either time domain [13] or frequency domain [6, 9]. Since a linear system can only generate iso-frequency coupling (quantified by linear coherence or cross-correlation) between an input and the output, a nonlinear interaction can be easily detected in the frequency domain by measuring the input-output interaction across different frequencies [9, 11, 14-17]. Bicoherence and its variants are often used frequency domain methods for probing nonlinear interactions in the nervous system [15, 18, 19]. A second-order nonlinearity, such as $y = x^2$, can be easily identified by bicoherence using a stimulus containing at least two different frequencies [16]. For example, Shils *et al* (1996) applied bicoherence to identify the second-order nonlinear interactions in the human visual system with a bi-frequency stimulus [15]. However, bicoherence cannot detect nonlinear

interactions beyond the second order, neither the high-order intermodulation/harmonic coupling nor the subharmonic coupling.

Subharmonic coupling is typically assessed by phase synchrony (PS) measures such as the n:m phase synchronization index [20]. However, PS measures assess nonlinear interactions (as well as linear interactions) between two signals purely based on their relative phase, independent of signal amplitude (see [20, 21] for details and [22] for a review). Therefore, they are more often used to investigate the synchronized discharge of neuronal populations (e.g. functional connectivity between brain areas) than estimating input-output relation regarding both phase and amplitude.

Thus, there is a need for a general nonlinear coherence framework that can quantify the different types of nonlinear input-output interaction and incorporates not only *phase* but also *amplitude* relation between the input and the output of a system. Doing this, we will be able to identify the nonlinear characteristics of the nervous system in a more complete way than with existing measures.

The goal of this paper is to introduce a generalized coherence framework in the frequency domain for detecting and characterizing nonlinear stimulus-response interactions in the nervous system, namely cross-spectral coherence (CSC). CSC can detect different types of nonlinear interactions including harmonic and intermodulation coupling as present in static nonlinearities and also subharmonics, which only occur due to dynamic nonlinearities.

We developed two metrics under the CSC framework: 1) *n:m coherence*, for measuring harmonic and subharmonic coupling related to individual input frequencies, and 2) *multi-spectral coherence*, for quantifying intermodulation coupling among multiple (≥ 2) input frequencies.

A preliminary version of part of this work has been briefly reported in [23, 24] using a *single-subject* dataset. In this paper, we provide a thorough mathematical description of the proposed method. We verify the performance of the two CSC metrics first in model simulations involving both static and dynamic nonlinear systems. Then, we demonstrate the application of CSC for investigating the nonlinear stimulus-response relation in the human proprioceptive system during a motor control task. This dataset involves 11 healthy subjects. A multi-sine wrist movement was imposed (proprioceptive stimulus) while the subjects performed an isotonic wrist flexion. The brain responses were measured by EEG. In contrast with our previous work [23, 24], this study reports for the first time subharmonic coupling in the human proprioceptive system.

II. METHODS

First we summarize two types of nonlinear mapping from the input spectral components to the output spectral components, i.e. n:m mapping and integer multiplication mapping, to mathematically demonstrate how harmonic, subharmonic and intermodulation couplings are present in the frequency domain. Then, we introduce the CSC as a generalized framework for quantifying the corresponding nonlinear coupling. Simulations

are used to evaluate the proposed method. At the end of this section, we provide a description of the experimental dataset and signal processing to demonstrate an application of CSC to the human proprioceptive system.

A. Nonlinear Mapping

Let $X(f)$ and $Y(f)$ be the Fourier transforms of the input $x(t)$ and the output $y(t)$ signals. The nonlinear mapping from the input to the output in the frequency domain can be presented in two different ways:

1) *n:m mapping*:

$$Y^m(f_{out}) = H(n:m)\, X^n(f_{in}); \quad X^n \equiv \underbrace{XX\cdots X}_{n} \qquad (1)$$

where the output frequencies (f_{out}) are related to the input frequencies (f_{in}) by the ratio n/m (n and m are *coprime* positive integers), and $H(n:m)$ is the n:m mapping function. The n:m mapping can generate harmonic ($m = 1$) and subharmonic coupling ($m > 1$) between the input and the output in the frequency domain. Subharmonic coupling is typically present in a dynamic nonlinear system involving differential operations, such as the Duffing oscillator [25].

2) *Integer multiplication mapping*: the output component is an integer product of the input components at frequencies $f_1, f_2, \ldots, f_R$ ($f_1 < f_2 < \ldots < f_R$) with the integer powers $a_1, a_2, \ldots, a_R$:

$$Y(f_{out}) = H(f_1, f_2, \ldots f_R; a_1, a_2, \ldots, a_R)_d\, Q! \prod_{r=1}^{R} X^{a_r}(f_r) \qquad (2)$$

where

$$X^{a_r}(f_r) = \begin{cases} \underbrace{X(f_r)X(f_r)\cdots X(f_r)}_{a_r} & a_r > 0 \\ 1 & a_r = 0, \\ \underbrace{X^*(f_r)X^*(f_r)\cdots X^*(f_r)}_{|a_r|} & a_r < 0 \end{cases}$$

'*' indicates complex conjugate, the output frequency $f_{out} = \sum_{r=1}^{R} a_r f_r > 0$, $H(f_1, f_2, \ldots, f_R; a_1, a_2, \ldots, a_R)_d$ is a d-th order nonlinear mapping function for corresponding input frequencies and their weights, and Q is the number of non-zero a_r. The sum of the absolute values of integer powers is equal to the order of integer multiplication mapping: $d = \sum_{r=1}^{R} |a_r| \geq 2$. Integer multiplication mapping can generate intermodulation coupling ($Q > 1$) as well as harmonic coupling ($Q = 1$) between the output and the input at the corresponding order. The integer multiplication mapping can occur in a static nonlinear system that does not contain differential operations, such as a power function ($y = x^d$), where the order of integer multiplication mapping corresponds to the order of nonlinearity (d).

B. Cross-spectral Coherence

Cross-spectral coherence (CSC) is a generalized framework that can assess various types of nonlinear input-output

interaction. According to two different types of nonlinear mapping, there are two basic metrics under CSC: (i) n:m coherence and (ii) multi-spectral coherence.

1) *n:m coherence* quantifies the nonlinear coupling generated by the n:m mapping including harmonic and subharmonic coupling, and it is defined as:

$$nmc(f_{in}, f_{out}) = \frac{|S_{xy}(f_{in}, f_{out})|}{\sqrt{S_{xx}^n(f_{in})S_{yy}^m(f_{out})}} \quad (3)$$

where $f_{out} : f_{in} = n : m$, $S_{xx}^n(f) = <X^n(f)(X^n(f))^*>$ is the *n*-th order *auto-spectra* ($<\cdot>$ represents the averaging over segments) and $S_{xy}(f_{in}, f_{out})$ is the *n:m cross-spectrum*:

$$S_{xy}(f_{in}, f_{out}) = <X^n(f_{in})(Y^m(f_{out}))^*> \quad (4)$$

2) *Multi-spectral coherence* measures the nonlinear coupling generated by the integer multiplication mapping, including harmonic and intermodulation coupling, and it is defined as:

$$msc(f_1, f_2, ...f_R; a_1, a_2, ..., a_R; f_{out})_d = \frac{|S_{xy}(f_1, f_2, ...f_R; a_1, a_2, ..., a_R)|}{\sqrt{\left(\prod_{r=1}^R S_{xx}^{|a_i|}(f_r)\right) S_{yy}(f_{out})}} \quad (5)$$

where $f_{out} = \sum_{r=1}^R a_r f_r > 0$, $S_{xy}(f_1, f_2, ...f_R; a_1, a_2, ..., a_R)$ is the *integer multiplication cross-spectrum*, which is a generalization of high-order cross-spectrum [26] by adding the integer parameters $a_1, a_2, ..., a_R$:

$$S_{xy}(f_1, f_2, ...f_R; a_1, a_2, ..., a_R; f_{out}) = <\prod_{r=1}^R X^{a_r}(f_r)Y^*(f_{out})> \quad (6)$$

Each harmonic/intermodulation frequency (output frequency f_{out}) is determined by the input frequencies f_r and their weights a_r ($r = 1, 2, ..., R$). Thus, multi-spectral coherence only has $2 \times R$ free variables (R input frequencies f_r and R corresponding a_r). It is known from the inputs to Eq. (5) that which frequencies constitute an harmonic/intermodulation with which a_r. According to the order of integer multiplication mapping, we can shrink the range of a_r by $\sum_{r=1}^R |a_r| = d$ for a given order of nonlinearity (d). Thus, the *d*-th order multi-spectral coherence can be used to detect the *d*-th order harmonic and intermodulation coupling.

With these two basic metrics, the CSC framework can detect different types of nonlinear coupling in the frequency domain, as well as linear coupling. Linear coupling can be considered as a special case of harmonic coupling, i.e. the first order harmonic coupling. Both the n:m coherence and the multi-spectral coherence can detect harmonic coupling. Nevertheless, n:m coherence cannot detect the intermodulation coupling, while multi-spectral coherence is blind to the subharmonic coupling. Thus they are complementary.

Mathematically, Equation (3) and (5) can be merged to get a general representation of CSC:

$$csc(f_1, f_2, ...f_R; a_1, a_2, ..., a_R; m)_d = \frac{|S_{xy}(f_1, f_2, ...f_R; a_1, a_2, ..., a_R; m)|}{\sqrt{\prod_{r=1}^R S_{xx}^{|a_i|}(f_r)S_{yy}^m(f_{out})}} \quad (7)$$

where:

$$S_{xy}(f_1, f_2, ...f_R; a_1, a_2, ..., a_R; m) = <\prod_{r=1}^R X^{a_r}(f_r)(Y^m(f_{out}))^*> \quad (8)$$

Similar to the existing coherence measures [15, 22, 27], CSC incorporates phase and amplitude relationships between the input and the output. The value of CSC is proportional to the strength of coupling. A zero value indicates no coupling at all. The normalization we used here is consistent with the conventional normalization of (linear) coherence and bicoherence [28]. Advantage of this normalization is that it is based on the "pure" spectral magnitude, independent of any coupling between signals; though the maximum value of CSC may exceed 1 when it is computed from a limited number of segments. However, this problem is negligible when the nonlinear coherence values are obtained from hundreds of signal segments [29]. Alternative normalization methods have been discussed in [30,31,38]. Although some of these methods are bounded to 1, most of them are affected by the coupling of signals [30]. Nonetheless, for a coherence measure, the statistical power for correctly rejecting the null-hypothesis is more important than the upper boundary. The comparison between different types of normalization, including the conventional type we used here, has concluded an essentially equal statistical power for all types [30]. The statistics are proven to be identical for all nonlinear coherence when the conventional normalization is applied [31]. Similar to bicoherence, estimates of magnitude squared CSC (csc^2) for Gaussian noise are approximately *chi-squared* distributed with degree of freedom $2N$ for N segments. The bias for cross-spectral coherence is $\sqrt{1/N}$ in this case, and the threshold for checking significant CSC values can be computed as $\sqrt{1 - p^{1/(N-1)}}$ when the true CSC lies with probability of $(1-p) \times 100\%$.

C. Model simulations

To verify the effectiveness of CSC, we simulated two different types of nonlinear systems, i.e. Duffing oscillator and a power function, to generate different types of nonlinear coupling. The n:m coherence was computed for detecting the harmonic and subharmonic coupling generated by the Duffing oscillator, while multi-spectral coherence was computed, for detecting the harmonic and intermodulation coupling produced by the power function. The confidence level was set with $p = 0.05$.

1) *Duffing oscillator* is a type of dynamic nonlinear system driven by a sine wave [25], which can generate output components at the harmonics and subharmonics of the driven frequency. The Duffing oscillator has been used to model the nonlinear dynamics in EEG for both cognitive
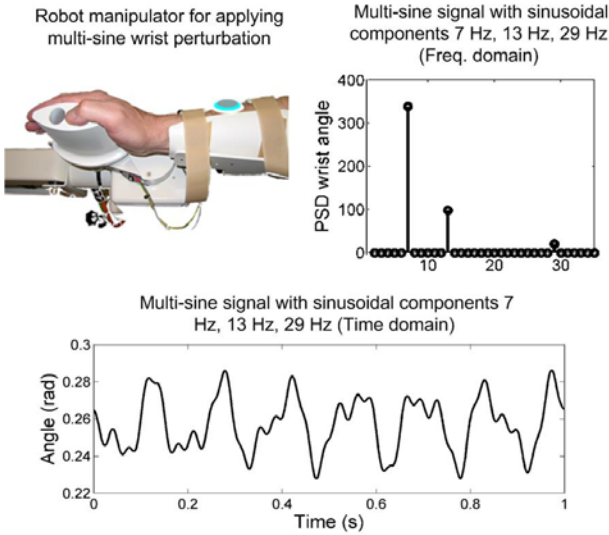
Fig.1. System input (proprioceptive): wrist manipulator and multi-sine perturbation.

and clinic studies [32-34]. A mathematical description of Duffing oscillator is given as:

$$\ddot{y} + \delta \dot{y} + \alpha y + \beta y^2 = x(t) \qquad (9)$$

where the driving force $x(t) = \gamma \cos(\omega t)$, the output $y = y(t)$ is the at time t, $\dot{y}$ is the first derivative of y with respect to time, *i.e. velocity*, $\ddot{y}$ is the second time-derivative of y, *i.e. acceleration*. The parameter δ controls the damping, α controls the stiffness, and β controls the amount of non-linearity in the restoring force. For testing n:m coherence, the duffing oscillator was simulated with $\delta = 0.2$, $\alpha = 1$, $\beta = 0.1$ and $x(t) = 8\cos(2t)$ with 2400 periods (sampling rate 80 rad/s = 40/π Hz). White noise was added to the output signal (SNR = –15dB) to represent measurement noise. To detect the harmonic and subharmonic coupling, we compute the n:m coherence with 600 non-overlapping segments. Each segment contained 4 periods (4π s). So the frequency resolution of n:m coherence was 1/4 rad/s (= 1/8π Hz).

2) *Power function* $(y = x^d)$ is a nonlinear system, which can produce harmonic and intermodulation coupling between the input and the output when using a multi-sine signal (sum of sine waves) as the input. According to Friston's review, most input-output relationship in neural systems can be approximately described by Volterra series, which is a polynomial power series containing different order of nonlinear terms [35]. The monomial power function $y = x^d$ is the basic element of polynomial representations of nonlinear systems. Compared to other nonlinear models, the advantage of the power function is that it generates harmonic and intermodulation coupling between the input and the output in the same order as its power d. For testing multi-spectral coherence, the system was stimulated for $d = 3$ (cubic function), and a multi-sine signal consisting of three sinusoids (7, 13, 29 Hz) with randomly chosen phases and 600 periods (period 1 s, sampling rate 256 Hz).

These three frequencies were chosen to avoid any overlap of the second-order and third-order harmonic and intermodulation frequencies. In this case, the second-order and third-order multi-spectral coherence results can be plotted as a discrete spectrum of the output frequencies. White noise was added to the output signal (SNR = –15 dB) to represent the measurement noise. For comparison, we computed the second-order (bicoherence) and the third-order multi-spectral coherence, with 600 non-overlapping segments. Each segment contained one period (1 s). So the frequency resolution of multi-spectral coherence was 1 Hz.

D. Application to the human proprioceptive system

We used the CSC framework to investigate the nonlinear interactions in the human proprioceptive system during a motor control task. The datasets were recorded from eleven subjects who performed isotonic *right* wrist flexions (1 Nm) while receiving a multi-sine position (angular) perturbation on the same wrist (see Fig. 1.). The perturbation signal consisted of a sum of three sine waves with the frequencies 7, 13, and 29 Hz and random phases. The magnitude of the sinusoids decreased with frequency to keep the same power per frequency in the velocity signal [36]. The period of the perturbation signal was 1 s, and the peak-to-peak amplitude was 0.06 rad. The experiment consisted of 60 trials with a 22 s task period in each trial with 1-s fade-in and fade-out periods. Detailed information about this dataset is available in [46].

The EEG were recorded using a 128-channel cap (5/10 systems, WaveGuard, ANT Neuro, Germany) with Ag/AgCl electrodes, using a common average reference. The EEG, the perturbation and the torque signals were digitalized at 2048 Hz using a Refa amplifier (Twente Medical Systems International B.V., the Netherlands) and stored for offline analysis. We removed the first 3 s and the last 2 s of each trial to exclude transient responses. To study the nonlinear interactions between the perturbation and the EEG, all data were segmented into 6-s segments with 5-s overlap. The length of the segments allows to detect potential subharmonics $k \cdot (f/2, f/3, f/6)$ reported in the literature [11, 37]. The use of overlapping segments not only increases the number of segments [38] but also reduces the bias and variance of the coherence estimates [39]. Segments contaminated by artefacts in the EEG (e.g. blinking and eye movements) were removed by visual inspection. After artefact removal, we obtained more than 500 segments for each subject. This amount of data has been proven to be sufficient for a reliable nonlinear coherence analysis in EEG [38]. All data were transformed to the frequency domain by fast Fourier transform using the function fft.m from MATLAB. The n:m coherence and multi-spectral coherence were computed between the perturbation and the EEG at channel C3 (around the left sensorimotor area) to investigate the stimulus-response relation. The multi-spectral coherence is computed up to the third order, since the frequencies of stimulation allow to exclusively assess all second-order and third-order nonlinearities without overlap in the output (EEG) spectrum. Since the non-stationary properties of the EEG signal may affect the estimation of nonlinear coherence [40], we performed

a 10-fold cross-validation to get the 95% confidence interval (mean ± 2std.) of the estimated CSC values. In each fold of the cross-validation we randomly picked out 90% of the signal segments to compute CSC values. This was repeated 10 times to estimate the mean and standard deviation of CSC. We considered the results as significant only when the lower boundary of the interval was higher than the significant threshold. Additionally, Bonferroni correction was applied to control for type I error, since we scanned EEG spectrum from 1-100 Hz. Thus, the significant threshold was adapted with p/100=0.0005 for 5% family-wise error rate.

III. RESULTS

A. Simulations

Fig. 2. and Fig. 3. show example periods of the input $x(t)$ and the output signals $y(t)$ and the amplitude spectra $|X(f)|$ and $|Y(f)|$ of the Duffing oscillator and the cubic function in noise-free cases. The Duffing oscillator generated output spectral components in the subharmonics ($f_{in}/2 = 1$ rad/s and $3f_{in}/2 = 3/2$ rad/s) and first-order harmonic of the driven frequency ($f_{in} = 2$ rad/s) in the examined frequency range. The cubic function produced output spectral component in third-order harmonics and intermodulations of the input frequencies.
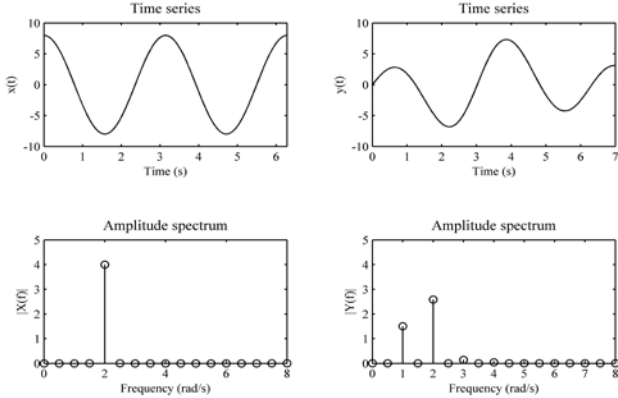

Fig.2. Input and output of the simulated Duffing oscillator (noise-free case). This system generated spectral components in the subharmonic frequencies (1 and 3 rad/s) and the first-order harmonic of the driven frequency (2 rad/s).
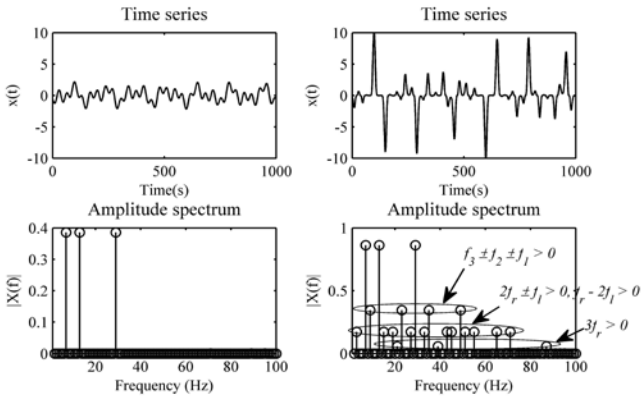

Fig.3. Input and output in the cubic function (noise-free case). Left column: Input signal containing three base frequencies 7, 13 and 29 Hz. Right column: Cubic function produced output spectral component in the third-order harmonics ($3f_r$: 21, 39 and 87 Hz), intermodulation between two frequencies ($2f_r \pm f_i$: 1, 19, 27, 33, 43, 45, 51, 55, 65 and 71 Hz; $f_r - 2f_i$: 3 and 5 Hz), intermodulation among three frequencies ($f_3 \pm f_2 \pm f_1$: 9, 23, 35, 49 Hz) and the base frequencies (7, 13 and 29 Hz).

Fig. 4. shows the results of the n:m coherence (Fig. 4a) and multi-spectral coherence (Fig. 4b) for the Duffing oscillator and the cubic function, respectively (SNR = - 15 dB). Significant n:m coherence is shown in the corresponding subharmonics (1 rad/s and 3 rad/s) and harmonic (2 rad/s) for the Duffing oscillator. Only the third-order multi-spectral coherence is significant for the cubic function. These results demonstrate that the n:m coherence can detect the subharmonic and harmonic coupling, while a given order multi-spectral coherence can detect the corresponding order harmonic and intermodulation coupling. Noteworthy, the magnitudes of both nonlinear coherences are in line with the amplitude spectrum of the output when the noise level is the same for all frequencies. Thus CSC can reflect the effect of signal amplitude in the input-output relation.
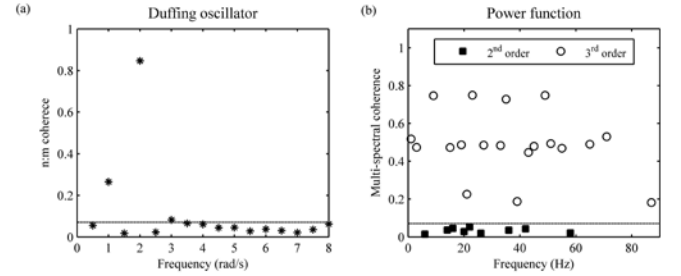

Fig.4. CSC analysis results in simulation test (SNR = -15 dB). Results are plotted as discrete spectra of the output frequencies. Horizontal lines indicate the significant levels (600 segments). (a) n:m coherence for the Duffing oscillator. The significant values are shown in 1 rad/s, 2 rad/s and 3 rad/s. (b) multi-spectral coherence for the cubic function. Significant value are shown in the third-order harmonics and intermodulations. All second-order harmonic and intermodulation values (bicoherence) are not significant.

B. Application to the human proprioceptive system

The results of n:m coherence and multi-spectral coherence are shown in Figs. 5 to 8 for an example subject (Subject 10, number of data segments: 942). In line with a previous study [36], the linear interaction (the first order harmonic coupling) was shown between the perturbation and EEG. High order (≥ 2) harmonic and intermodulation couplings were detected for this subject, as well as subharmonic coupling for 29 Hz (1:2).
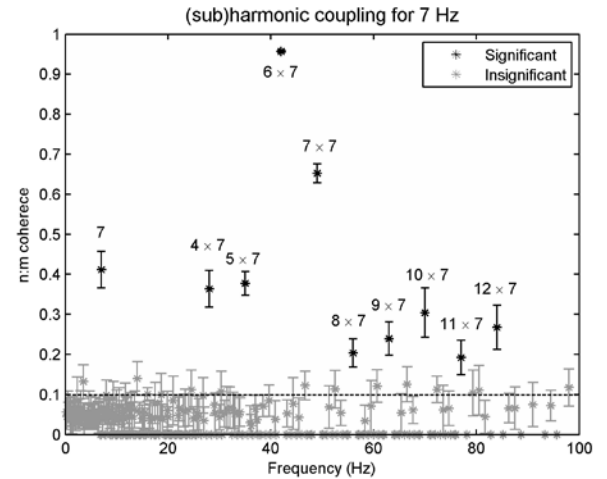

Fig.5. n:m coherence for the 7 Hz input frequency component. Error bars show the 95% confidential interval of the coherence values estimated by 10-fold cross-validation. Horizontal line indicates the Bonferroni corrected significant level (942 segments). Only significant harmonic coupling is detected.
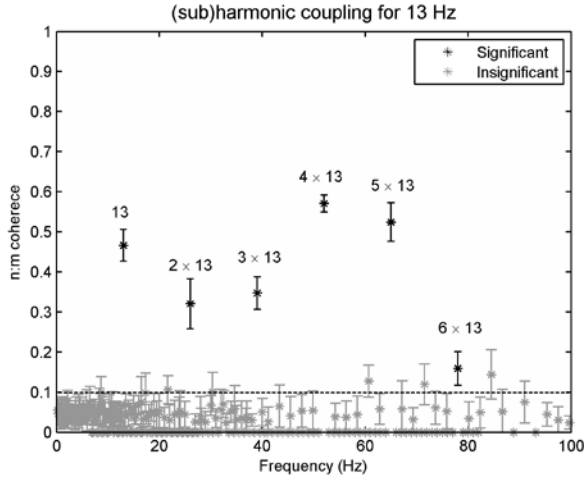
6

Fig.6. n:m coherence for the 13 Hz input frequency component. Error bars show the 95% confidential interval of the coherence values. Horizontal line indicates the Bonferroni corrected significant level. Only significant harmonic couplings are detected.
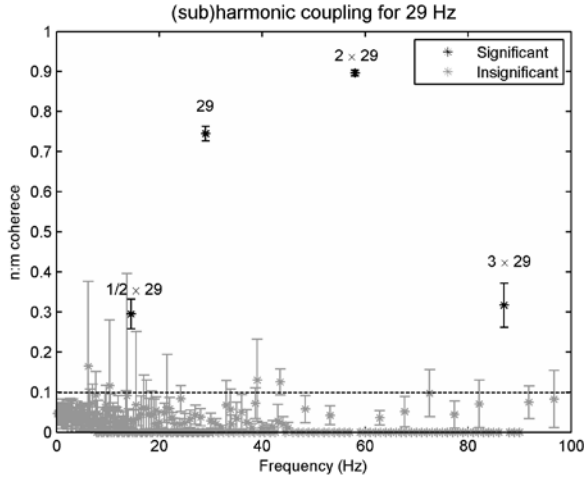

Fig.7. n:m coherence for the 29 Hz input frequency component. Error bars show the 95% confidential interval of the coherence values. Horizontal line indicates the Bonferroni corrected significant level. Significant subharmonic (1:2) and harmonic couplings are detected.
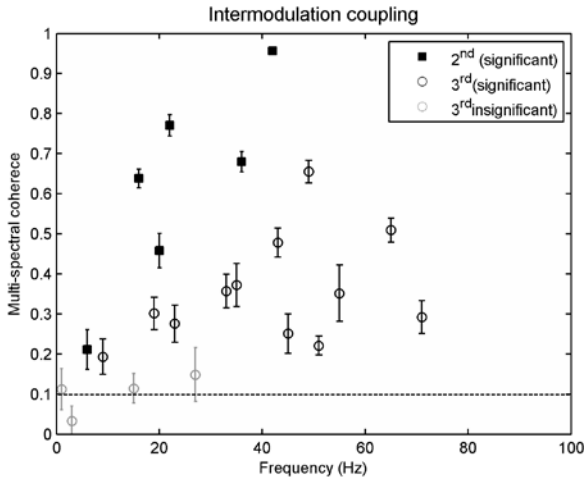

Fig.8. Multi-spectral coherence. Error bars show the 95% confidential interval of the coherence values. Horizontal line indicates the Bonferroni corrected significant level. To avoid the information redundancy with the results from n:m coherence, we only present intermodulation coupling results. Significant intermodulation coupling is detected in the second (squares) and third (circles) orders.
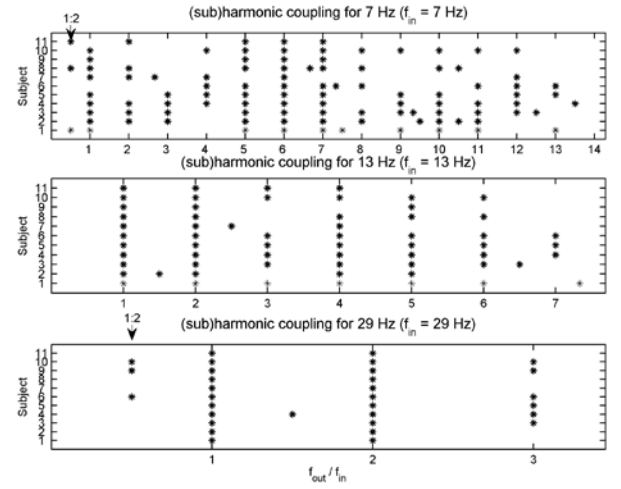

Fig.9. n:m coherence for each input frequency for all subjects. Only the significant results are indicated (stars). Results are shown as discrete spectra of frequency ratio f_{out}/f_{in} (= n:m). Integer ratios (m = 1) correspond to different order harmonics, non-integer ratios correspond to subharmonics.
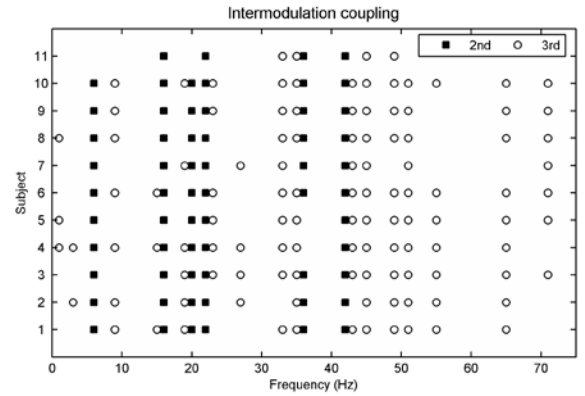

Fig.10. Multi-spectral coherence for all subjects. Only the significant second-order (squares) and third-order (circles) intermodulation couplings are presented as the discrete spectra of the output frequencies.

Fig. 9 and Fig. 10 summarize the group results. High order harmonic and intermodulation couplings were found in all subjects, despite individual differences of the output frequencies. Subharmonic coupling was shown in 8 out of 11 subjects. In particularly, subharmonic 1:2 was detected in three subjects with the frequency 7 Hz, and in three additional subjects with the frequency 29 Hz.

IV. DISCUSSIONS

As an extension of nonlinear coherence measures (bicoherence and its variants), the CSC framework can assess nonlinear interactions in static nonlinearities, i.e. harmonic and intermodulation coupling, and nonlinear interactions *exclusively* due to dynamic nonlinearities, i.e. subharmonic coupling. Additionally, the CSC framework can also quantify the linear interaction (as the first order harmonic coupling). Thus, the CSC framework provides a more complete description of input-output interactions in the nervous system than existing coherence measures (linear coherence and bicoherence). Different from generalized phase synchrony measures [20, 21], the CSC framework reflects not only phase but also amplitude relation between the input and the output;

therefore the CSC framework is more suitable for probing stimulus-response interactions regarding both phase and amplitude relation in the nervous system [21]. For researchers who are interested in phase synchrony, please refer to our recent work in [21].

We introduced two different types of nonlinear mapping from the input to the output in the frequency domain, namely n:m mapping and integer multiplication mapping. The n:m mapping can occur in a dynamic nonlinear system, such as a Duffing oscillator, which can generate subharmonic coupling, as well as harmonic coupling. The integer multiplication mapping can be present in a static nonlinear system, such as a power function, which cannot yield subharmonic coupling. When the input is a signal containing a reduced number of specific frequency components (e.g. a multi-sine signal), integer multiplication mapping can produce intermodulation coupling among multiple input frequencies. According to these two types of nonlinear mapping, we introduced two metrics under the CSC framework, namely n:m coherence and multi-spectral coherence to assess different types of nonlinear interactions. A practical approach to probing nonlinear interactions in the human nervous system is to perturb the system using a periodic steady-state sensory stimulus (e.g. single-sine or multi-sine stimuli) [11, 24]. By measuring EEG, one can get the neural response to investigate the nonlinear stimulus-response relation in the central nervous system.

By using a multi-sine wrist perturbation, we demonstrated the application of the CSC framework to investigate the human proprioceptive system. Compared to previous studies using single-sine stimuli [7, 11], multi-sine stimulus can evoke richer nonlinearity including the intermodulation coupling among multiple stimulation frequencies [17, 21]. In line with previous studies [14, 21, 41], intermodulation and harmonic couplings were detected in all subjects, indicating that integer multiplication mapping is an important nonlinear mapping in the system. Nevertheless, this indication alone does not mean the proprioceptive system is static, since in this study subharmonic coupling was also found in the majority of the subjects (8 out of 11).

Subharmonic coupling between brain responses and steady-state sensory stimuli (e.g. visual flickering) has often been reported in the human visual system [3, 7]. Most studies using somatosensory stimuli, mainly using tactile stimuli,) only reported harmonic and intermodulation coupling (see [8, 10, 14, 36, 41] for examples and a brief review is available in [42]). To the best of our knowledge, only Langdon and his colleagues has reported 2:3 subharmonic coupling between brain responses and tactile vibrations [11]. There are only a very few previous studies investigating nonlinear interactions between brain responses and proprioceptive stimuli [21, 23, 24, 42]. None of them has reported subharmonic coupling. Subharmonic coupling is typically associated with a complex nonlinear dynamics in a system showing *bifurcations* [12]. This kind of system is mediated by the bifurcation parameters such as the amplitude of the driving force (here the intensity of stimulus). If this kind of nonlinear system is mildly excited, then the response will be steady-state and only contain spectral

components in the harmonic and intermodulation frequencies (see [12] for details). Subharmonic coupling can only be detected in the nervous system when the bifurcation parameters are in the range that a severely nonlinear behavior (e.g. multi-stability) is shown [3, 12, 43].

To allow examination of the spectral component at subharmonics of the driven frequency, the frequency resolution of data analysis should be fine enough, and the analyzing method needs be suitable for detecting the subharmonic coupling. These conditions may not always be satisfied in previous studies. For example, the method used in [21] can only detect *phase* coupling in harmonic and intermodulation; and the frequency resolution of data analysis in [23, 24] is not fine enough for detecting subharmonics. The movement perturbation used in [42] has a smaller peak-to-peak value and contains only low frequency components. These differences may explain why subharmonic coupling was not detected in the previous studies but shown in this study.

In a nonlinear system showing bifurcations, the values of bifurcation parameters at which the stability of an equilibrium changes (e.g. from steady state to multi-stability) are known as the bifurcation points [12]. Considering individual differences, the bifurcation points in the human proprioceptive system could vary between subjects, which could explain why subharmonic coupling was not shown in all subjects. Similar to the previous findings in the human visual system [3, 7], 1:2 subharmonic coupling was the most common subharmonic coupling. In this study, we did not find 2:3 subharmonic coupling. The difference in the ratio of subharmonic coupling between subjects further indicates complex nonlinear dynamics in the human proprioceptive system. Since sensory information projected to the cortex via thalamus, the nonlinear coupling between the stimulus and cortical response could be mediated by both the external stimulus and the internal dynamics of the thalamo-cortical populations [44, 45]. As such, highly complex nonlinear dynamics could be generated [3].

V. CONCLUSION

This work introduces a general nonlinear coherence framework for probing nonlinear interactions in the nervous system. The cross-spectral coherence (CSC) framework can detect nonlinear input-output interactions in the frequency domain, indicated as harmonic, subharmonic and intermodulation coupling, for both static and dynamic nonlinearities. The application of the CSC framework to a motor control dataset reports for the first time subharmonic coupling between stimulus and EEG response, indicating a complex nonlinear dynamics in human proprioceptive system. Our empirical findings provide a more complete description of nonlinear dynamics in the human proprioceptive system and could be a critical pre-requisite for system identification and parameter estimation of the human proprioceptive system.

Preliminary versions of part of this work were presented in the 2nd International Conference on Basic and Clinical multimodal Imaging, Utrecht, the Netherlands [27], and the 17th IFAC Symposium on System Identification, Beijing, China [26]; and benefited from the discussions with Guido Nolte, Ole Jensen and Johan Schoukens.

REFERENCES

[1] E. Pereda et al., "Nonlinear multivariate analysis of neurophysiological signals," *Prog. Neurobiol.,* vol. 77, no. 1, pp. 1-37, Oct. 2005.

[2] A. Spiegler et al., "Modeling brain resonance phenomena using a neural mass model," *PLoS Comupt. Biol.,* vol. 7, no. 12, pp. e1002298, Dec. 2011.

[3] J. Roberts, and P. Robinson, "Quantitative theory of driven nonlinear brain dynamics," *Neuroimage,* vol. 62, no. 3, pp. 1947-1955, Sep. 2012.

[4] T. D. Sanger et al., "Nonlinear sensory cortex response to simultaneous tactile stimuli in writer's cramp," *Mov. Disord.,* vol. 17, no. 1, pp. 105-111, Jan. 2002.

[5] T. Nyrke, and A. Lang, "Spectral analysis of visual potentials evoked by sine wave modulated light in migraine," *Electroencephalogr. Clin. Neurophysiol.,* vol. 53, no. 4, pp. 436-442, Apr. 1982.

[6] S. Kalitzin et al., "Enhancement of phase clustering in the EEG/MEG gamma frequency band anticipates transitions to paroxysmal epileptiform activity in epileptic patients with known visual sensitivity," *IEEE Trans. Biomed. Eng.,* vol. 49, no. 11, pp. 1279-1286, Nov. 2002.

[7] C. S. Herrmann, "Human EEG responses to 1–100 Hz flicker: resonance phenomena in visual cortex and their potential correlation to cognitive phenomena," *Exp. Brain Res.,* vol. 137, no. 3-4, pp. 346-353, Apr. 2001.

[8] A. Z. Snyder, "Steady-state vibration evoked potentials: description of technique and characterization of responses," *Electroencephalogr. Clin. Neurophysiol.,* vol. 84, no. 3, pp. 257-268, 1992.

[9] M. Regan, and D. Regan, "A frequency domain technique for characterizing nonlinearities in biological systems," *J. Theor. Biol.,* vol. 133, no. 3, pp. 293-317, Aug. 1988.

[10] S. Jamali, and B. Ross, "Somatotopic finger mapping using MEG: toward an optimal stimulation paradigm," *Clin. Neurophysiol.,* vol. 124, no. 8, pp. 1659-1670, Aug. 2013.

[11] A. J. Langdon et al., "Multi-frequency phase locking in human somatosensory cortex," *Prog. Biophys. Mol. Biol,* vol. 105, no. 1, pp. 58-66, Mar. 2011.

[12] S. A. Billings, *Nonlinear system identification: NARMAX methods in the time, frequency, and spatio-temporal domains*: John Wiley & Sons, 2013.

[13] F. L. da Silva et al., "Interdependence of EEG signals: linear vs. nonlinear associations and the significance of time delays and phase shifts," *Brain Topogr.,* vol. 2, no. 1-2, pp. 9-18, Sep. 1989.

[14] B. Ross et al., "Synchronization of beta and gamma oscillations in the somatosensory evoked neuromagnetic steady-state response," *Exp. Neurol.,* vol. 245, pp. 40-51, Jul. 2013.

[15] J. Shils et al., "Bispectral analysis of visual interactions in humans," *Electroencephalogr. Clin. Neurophysiol.,* vol. 98, no. 2, pp. 113-125, Feb. 1996.

[16] J. C. Sigl, and N. G. Chamoun, "An introduction to bispectral analysis for the electroencephalogram," *J. Clin. Monit.,* vol. 10, no. 6, pp. 392-404, Nov. 1994.

[17] J. Victor, and R. Shapley, "A method of nonlinear analysis in the frequency domain," *Biophys. J.,* vol. 29, no. 3, pp. 459, Mar. 1980.

[18] F. Chella et al., "Third order spectral analysis robust to mixing artifacts for mapping cross-frequency interactions in EEG/MEG," *NeuroImage,* vol. 91, pp. 146-161, May 2014.

[19] F. Darvas et al., "Bi-phase locking—a tool for probing non-linear interaction in the human brain," *NeuroImage,* vol. 46, no. 1, pp. 123-132, May. 2009.

[20] P. Tass et al., "Detection of n: m phase locking from noisy data: application to magnetoencephalography," *Phys. Rev. Lett.,* vol. 81, no. 15, pp. 3291, Oct. 1998.

[21] Y. Yang et al., "A general approach for quantifying nonlinear connectivity in the nervous system based on phase coupling," *Int. J. Neural Syst.,* vol. 26, no. 1, pp. 1550031, Feb. 2016.

[22] C. K. Young, and J. J. Eggermont, "Coupling of mesoscopic brain oscillations: recent advances in analytical and theoretical perspectives," *Prog. Neurobiol.,* vol. 89, no. 1, pp. 61-78, Sep. 2009.

[23] Y. Yang et al., "Probing the Nonlinearity in Neural Systems Using Cross-frequency Coherence Framework," *IFAC-PapersOnLine*, vol.48, no.28, pp. 1386-1390, Dec. 2015.

[24] Y. Yang et al., "Multi-Sine Stimuli are a Powerful Tool for Imaging Nonlinearity in Nervous Systems," presented at 2nd Int. Conf. Basic & Clinical Multimodal Imaging, Utrecht, The Netherlands, Sep 1-5, 2015.

[25] M. E. Levenson, "Harmonic and Subharmonic Response for the Duffing Equation ẍ+ αx+ βx3= F cosωt (α> 0)," *J. Appl. Phys.,* vol. 20, no. 11, pp. 1045-1051, Nov. 1949.

[26] C. L. Nikias, and J. M. Mendel, "Signal processing with higher-order spectra," *IEEE Signal Process. Mag.,* vol. 10, no. 3, pp. 10-37, Jul. 1993.

[27] R. A. Dobie, and M. J. Wilson, "Objective detection of 40 Hz auditory evoked potentials: phase coherence vs. magnitude-squared coherence," *Electroencephalogr. Clin. Neurophysiol.,* vol. 92, no. 5, pp. 405-413, Sep. 1994.

[28] D. R. Brillinger, "An introduction to polyspectra," *Ann. Math. Stat.*, pp. 1351-1374, Oct. 1965.

[29] S. Elgar, and R. Guza, "Statistics of bicoherence," *IEEE Trans Acoust,* vol. 36, no. 10, pp. 1667-1668, Oct. 1988.

[30] F. Shahbazi et al., "Univariate normalization of bispectrum using Hölder's inequality," *J. Neurosci. Meth.,* vol. 233, pp. 177-186, Aug. 2014.

[31] V. Chandran et al., "Statistics of tricoherence," *Signal Processing, IEEE Transactions on,* vol. 42, no. 12, pp. 3430-3440, Dec. 1994.

[32] N. J. Stevenson et al., "A nonlinear model of newborn EEG with nonstationary inputs," *Ann. Biomed Eng.,* vol. 38, no. 9, pp. 3010-3021, Sep. 2010.

[33] R. Srebro, "The Duffing oscillator: a model for the dynamics of the neuronal groups comprising the transient evoked potential," *Electroencephalogr. Clin. Neurophysiol.,* vol. 96, no. 6, pp. 561-573, Nov. 1995.

[34] H. Witte et al., "Analysis and modeling of time-variant amplitude–frequency couplings of and between oscillations of EEG bursts," *Biological Cybernetics,* vol. 99, no. 2, pp. 139-157, Aug. 2008.

[35] K. J. Friston, "Brain Function, Nonlinear Coupling, and Neuronal Transients," *The Neuroscientist,* vol. 7, no. 5, pp. 406-418, Oct. 2001.

[36] S. F. Campfens et al., "Quantifying connectivity via efferent and afferent pathways in motor control using coherence measures and joint position perturbations," *Exp. Brain Res.,* vol. 228, no. 2, pp. 141-153, Jul. 2013.

[37] A. Daffertshofer et al., "Spatio-temporal patterns of encephalographic signals during polyrhythmic tapping," *Hum. Movement Sci.,* vol. 19, no. 4, pp. 475-498, Oct. 2000.

[38] S. Hagihira et al., "Practical issues in bispectral analysis of electroencephalographic signals," *Anesth. Analg.,* vol. 93, no. 4, pp. 966-970, Oct. 2001.

[39] R. Bortel, and P. Sovka, "Approximation of statistical distribution of magnitude squared coherence estimated with segment overlapping," *Signal Process.,* vol. 87, no. 5, pp. 1100-1117, May 2007.

[40] J.-P. Lachaux et al., "Measuring phase synchrony in brain signals," *Hum. Brain Mapp.,* vol. 8, no. 4, pp. 194-208, Jan. 1999.

[41] S. Tobimatsu et al., "Steady-state vibration somatosensory evoked potentials: physiological characteristics and tuning function," *Clin. Neurophysiol.,* vol. 110, no. 11, pp. 1953-1958, Nov. 1999.

[42] M. P. Vlaar et al., "Frequency Domain Characterization of the Somatosensory Steady State Response in Electroencephalography," *IFAC-PapersOnLine,* vol. 48, no. 28, pp. 1391-1396, Dec. 2015.

[43] S. Kalitzin et al., "Multiple oscillatory states in models of collective neuronal dynamics," *Int. J. Neural Syst.,* vol. 24, no. 06, pp. 1450020, Sep. 2014.

[44] M. Breakspear, "User Research Multi-stability and non-linearity of large-scale cortical rhythms," *Brain,* vol. 38, pp. 27, Mar. 2011.

[45] S. Makeig et al., "Mining event-related brain dynamics," *Trends Cogn. Sci.,* vol. 8, no. 5, pp. 204-210, May 2004.

[46] Y. Yang et al., "Nonlinear Connectivity in the Human Stretch Reflex Assessed by Cross-frequency Phase Coupling," *Int. J. Neural Syst.,* to be published, doi: 10.1142/S012906571650043X.

Yuan Yang received his Bachelor's Degree (top 5%) in biomedical engineering from Central South University, China in 2008, Master degree (honor student) in biomedical engineering from Shanghai Jiaotong University, China in 2010 and PhD degree (Très honorable) in signal and image processing from Télécom ParisTech (ENST) / CNRS LTCI, France in 2013. He has been a postdoctoral researcher at the Delft University of Technology, Delft, The Netherlands since Nov. 2013. His research experiences include biomedical signal processing, human movement control, brain-computer interfaces and face recognition. His current research focuses on nonlinear system identification, coherence and connectivity, complex brain network, EEG source localization and motor control.

Teodoro Solis-Escalante received a M.Sc. degree in biomedical engineering from the Universidad Autonoma Metropolitana-Iztapalapa, Mexico City, Mexico in 2007; and a Ph.D. degree in computer sciences from the Graz University of Technology, Graz, Austria in 2012. Currently, he is a postdoctoral researcher in the Laboratory for Neuromuscular Control at the Delft University of Technology, Delft, the Netherlands. His research interests include the human sensory and motor system, rehabilitation engineering, and brain–computer communication systems.

Frans C. T. van der Helm received the MSc degree in human movement science and the PhD degree in mechanical engineering, in 1985 and 1991, respectively. He is a professor in biomechatronics and bio-robotics, at the Delft University of Technology, and also an adjunct professor at the University of Twente and at Northwestern University in Chicago. He was a chair of the Dpartment of Biomechanical Engineering (2005- 2010). He was a member of the board of the International Society of Biomechanics (2005-2009), participates in the board of the Technical Group of Computer Simulation (TGCS), and the International Shoulder Group (ISG). He is one of the programme leaders in the Medical Delta and Principal Investigator in the TREND research consortium. He has published more than 100 papers in international journals on topics as biomechanics of the upper and lower extremity, neuromuscular control, eye biomechanics, pelvic floor biomechanics, human motion control, posture stability, etc.

Alfred C. Schouten received the MSc and PhD degrees in mechanical engineering from the Delft University of Technology, Delft, the Netherlands, in 1999 and 2004, respectively. He is currently an associate professor at the Delft University of Technology and the University of Twente, Enschede, the Netherlands. He is a co-founder of the Delft Laboratory for Neuromuscular Control. His research interests include the field of neuromuscular control and techniques to quantify the functional contribution of afferent feedback, neuromuscular modeling, haptic manipulators, and system identification. His research focuses on both able-bodied individuals and individuals suffering from movement disorders.